Formation of superheavy nuclei in $^{36}S + ^{238}U$ and $^{64}Ni + ^{238}U$ reactions

V. L. Litnevsky,[1,*] F. A. Ivanyuk,[2,†] G. I. Kosenko,[3,‡] and S. Chiba[4,§]

[1]*Omsk State Transport University, 644046 Omsk, Russia*
[2]*Institute for Nuclear Research, 03028 Kiev, Ukraine*
[3]*Omsk Tank Automotive Engineering Institute, 644098 Omsk, Russia*
[4]*Tokyo Institute of Technology, 152-8550 Tokyo, Japan*

(Received 16 February 2020; revised manuscript received 25 March 2020; accepted 2 June 2020; published 17 June 2020)

We describe the capture, fusion, fission, and evaporation residue formation cross sections of superheavy nuclei within the proposed earlier two-stage dynamical model. The approaching of the projectile nucleus to the target nucleus is described in the first stage of the model. In the second stage, the evolution of the system formed after the touching of the projectile and target nuclei is considered. The evolution of the system on both stages is described by the Langevin equations. The transport coefficients of these equations for the shape degrees of freedom are calculated within the microscopic linear-response theory. The mutual orientation of the colliding ions, the tunneling through the Coulomb barrier in the entrance channel and the shell effects in the potential energy on both stages of the calculations are taking into account. The obtained results are compared with the available experimental data and other theoretical predictions.

DOI: 10.1103/PhysRevC.101.064616

I. INTRODUCTION

One of the most interesting and intensively developing branches of nuclear physics is the synthesis of superheavy elements (SHEs). Unfortunately, reactions in which two nuclei that are spherical in the ground state collide with each other (the cold fusion reactions) have exhausted themselves. Further studies of superheavy elements involve the hot fusion reactions, in which a spherical projectile nucleus interacts with a heavy deformed target nucleus.

The theoretical models of such reactions have to take into account the shell structure of colliding nuclei (in order to reproduce the nonspherical shape of the target nucleus in the ground state). Also, the initial orientation of the target nucleus relative to the line, connecting the centers of mass of colliding nuclei, should be taken into account. Finally, the possibility of deformation of the nuclei during the collision must be taken into account.

In the present paper, the reactions $^{36}S + ^{238}U \to ^{274}Hs$ and $^{64}Ni + ^{238}U \to ^{302}120$ are investigated by using the two-stage dynamic stochastic model [1–3]. These reactions differ significantly from each other by the ratio of the masses and charges of the colliding nuclei. It is well known that, with increasing mass asymmetry of colliding nuclei, there is a noticeable increase in the compound nuclei formation cross section. Thus, the comparison of calculated results for the considered reactions with the experimental data allows us to judge the ability to apply the developed model to the analysis of a wider range of the SHE formation reactions.

II. THE MODEL

In the model used here, the time evolution of the system is described by the Langevin equations [4,5] for the collective coordinates $\mathbf{q}$ and corresponding momenta $\mathbf{p}$. For the compact system the collective parameters consist only of shape (deformation) parameters, $\mathbf{q} \equiv (\alpha, \alpha_1, \alpha_4)$. Parameters α, α_1, α_4 are deformation parameters used in the shape parametrizations based on the Cassini ovaloids [6]. Parameter α is responsible for the total elongation of the shape, α_1 for the mass asymmetry, and α_4 for the neck radius. The examples of nuclear shapes are shown in Fig. 1.

For the entrance channel, the collective parameters are the parameters of deformation of the target α_t and projectile α_p, the distance r between the centers of mass of colliding ions, and the orientation angle θ_t between the symmetry axis of the deformed target and the line connecting centers of mass of the colliding nuclei, $\mathbf{q} \equiv (r, \alpha_t, \alpha_p, \theta_t)$. For $\alpha < 0.5$ and all $\alpha_i = 0$ the Cassini ovaloids are very close to spheroids. Thus, in the entrance channel, only spheroidal deformations of the target and projectile are taken into account.

The deformation energy $E_{\rm def}^{(t)}$ and $E_{\rm def}^{(p)}$ of colliding ions and $E_{\rm def}$ of the combined system at $T = 0$ are defined within the macroscopic-microscopic method [7], $E_{\rm def} = E_{\rm LDM} + \delta E$. The shell correction δE to the liquid drop energy was calculated by the approach, as proposed by Strutinsky [8,9].

*vlad.lit@bk.ru
†ivanyuk@kinr.kiev.ua
‡kosenkophys@gmail.com
§chiba.satoshi@nr.titech.ac.jp

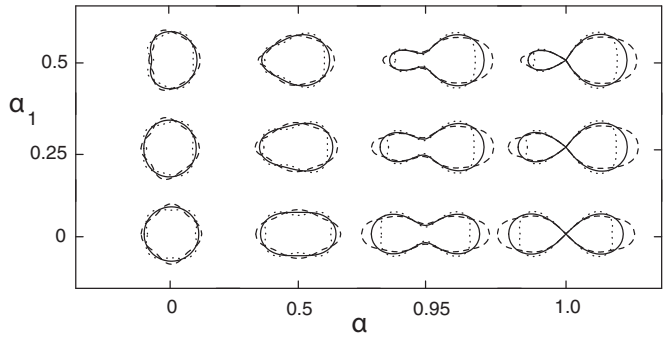

FIG. 1. The nuclear shapes versus α and α_1 at $\alpha_4 = -0.2$ (dotted lines), 0.0 (solid lines), and 0.2 (dashed lines).

The Langevin equations for **q** and **p** [4,5] are

$$\frac{dq_\mu}{dt} = (m^{-1})_{\mu\nu} p_\nu,$$

$$\frac{dp_\mu}{dt} = -\frac{\partial F(q,T)}{\partial q_\mu} - \frac{1}{2}\frac{\partial (m^{-1})_{\nu\sigma}}{\partial q_\mu} p_\nu p_\sigma - \gamma_{\mu\nu}(m^{-1})_{\nu\sigma} p_\sigma + g_{\mu\nu}\xi_\nu. \quad (1)$$

Here a convention of summation over repeated indices ν, σ is used. The quantity $\gamma_{\mu\nu}$ is the tensor of friction coefficients and $m_{\mu\nu}$ is the mass tensor,

At both stages of calculations the friction $\gamma_{\mu\nu}$ and inertia $m_{\mu\nu}$ tensors for the shape degrees of freedom are calculated within the linear-response approach and local harmonic approximation [10,11]. In this approach many quantum effects such as shell and pairing effects, and the dependence of the collisional width of the single-particle states on the excitation energy, are taken into account. For slow collective motion the tensors of friction $\gamma_{\mu\nu}$ and inertia $m_{\mu\nu}$ can be expressed in terms of first and second derivatives of the Fourier transform $\chi_{\mu\nu}(\omega)$ of the response function,

$$\chi_{\mu\nu}(\omega) = \sum_{kj} \xi_{kj}^2 \frac{n_k^T - n_j^T}{\hbar\omega - E_{kj}^- + i\Gamma_{kj}} F_{kj}^\mu F_{jk}^\nu + \sum_{kj} \eta_{kj}^2 \frac{n_k^T + n_j^T - 1}{\hbar\omega - E_{kj}^+ + i\Gamma_{kj}} F_{kj}^\mu F_{jk}^\nu, \quad (2)$$

$$\gamma_{\mu\nu} = -i\frac{\partial \chi_{\mu\nu}(\omega)}{\partial\omega}\Big|_{\omega=0}, \quad m_{\mu\nu} = \frac{1}{2}\frac{\partial^2 \chi_{\mu\nu}(\omega)}{\partial\omega^2}\Big|_{\omega=0}. \quad (3)$$

The precise expressions for the friction are

$$\gamma_{\mu\nu} = 2\hbar\sum_{kj}\left(n_j^T - n_k^T\right)\xi_{kj}^2 \frac{E_{kj}^-\Gamma_{kj}}{\left[(E_{kj}^-)^2 + \Gamma_{kj}^2\right]^2} F_{kj}^\mu F_{jk}^\nu + 2\sum_{kj}\left(1 - n_k^T - n_j^T\right)\eta_{kj}^2 \frac{E_{kj}^+\Gamma_{kj}}{\left[(E_{kj}^+)^2 + \Gamma_{kj}^2\right]^2} F_{kj}^\mu F_{jk}^\nu \quad (4)$$

and

$$m_{\mu\nu} = \hbar^2\sum_{kl}\left(n_j^T - n_k^T\right)\xi_{kj}^2 \frac{E_{kj}^-\left((E_{kj}^-)^2 - 3\Gamma_{kj}^2\right)}{\left[(E_{kj}^-)^2 + \Gamma_{kj}^2\right]^3} F_{kj}^\mu F_{jk}^\nu + \hbar^2\sum_{kj}\left(1 - n_k^T - n_j^T\right)\eta_{kj}^2 \frac{E_{kj}^+\left((E_{kj}^+)^2 - 3\Gamma_{kj}^2\right)}{\left[(E_{kj}^+)^2 + \Gamma_{kj}^2\right]^3} F_{kj}^\mu F_{jk}^\nu. \quad (5)$$

Here E_k, E_j are the energies of quasiparticle states in the ABCS-approximation, $E_{kj}^- \equiv E_k - E_j$, $E_{kj}^+ \equiv E_k + E_j$, $n_k^T \equiv 1/[1 + \exp(E_k/T)]$, $\eta_{kj} = u_k\upsilon_j + u_j\upsilon_k$, $\xi_{kj} = u_k u_j - \upsilon_k\upsilon_j$, where u_k, υ_k are the coefficients of the Bogoliubov-Valatin transformation. The operator F^μ, whose matrix elements F_{kj}^μ appear in Eqs. (4) and (5), is the derivative of the single-particle Hamiltonian with respect to the deformation parameter q_μ. The quantity Γ_{kj} is the average width of the two-quasiparticle states, $\Gamma_{kj} = [\Gamma(E_k, \Delta, T) + \Gamma(E_j, \Delta, T)]/2$. The calculation of Γ_{kj} for the system with pairing is explained in detail in Ref. [12]. One of us (F.I.) apologizes very much for the misprints in expressions for $\gamma_{\mu\nu}$ and $m_{\mu\nu}$, given in Ref. [13].

$F(q,T)$ in Eq. (1) is the free energy of the system. For the shape degrees of freedom, it is calculated as the sum of the liquid drop energy and the shell corrections (including the corrections to the pairing energy) for neutrons and protons,

$$F(q,T) = F_{LDM}(q) + \delta F^{(n)}(q,T) + \delta F^{(p)}(q,T), \quad (6)$$

with

$$F_{LDM}(q) = E_{LDM}(q) - \widetilde{a}T^2. \quad (7)$$

The damping of the shell corrections with the temperature was calculated according to Ignatyuk prescription [14],

$$\delta F(q,T) = \delta E(q, T=0)e^{-aT^2/E_d}, \quad E_d = 20\ \text{MeV}. \quad (8)$$

The temperature T was related to the local excitation (dissipated) energy $E^*(q)$ by the energy conservation condition at each time step of integration of Eqs. (1),

$$E^*(q) = E_x - \frac{1}{2}\sum_{\mu\nu}(m^{-1})_{\mu\nu} p_\mu p_\nu - V_{\text{pot}} = aT^2. \quad (9)$$

Here E_x is the initial excitation energy, see below. For the level-density parameters $\widetilde{a}$ and a we use the approximations from Ref. [15]:

$$\widetilde{a}(A) = \alpha A + \beta A^{2/3} B_S, \quad (10)$$

where B_S is the ratio of nuclear surface to the surface of spherical nucleus, and α and β are constants, and

$$a(A, E^*) = \widetilde{a}(A)[1 + \delta E(T=0)(1 - e^{-E^*/E_d})/E^*]. \quad (11)$$

Here the level-density parameter $a(A, E^*)$ clearly contains the shell effects. We do not subtract the pairing gap Δ from E^* since the pairing effects are already included both into δE and E^*.

The energy (6) depends only on the parameters of the shape of the nucleus. It does not depend on the distance between ions or their orientation in space. In the entrance channel the

nuclear $V_{\rm GK}(q)$ and Coulomb $V_{\rm Coul}(q)$ interactions between the ions should be added to the free energy (6),

$$F^I(q,T) = F^{(t)}(q,T) + F^{(p)}(q,T) + V_{\rm Coul}(q) + V_{\rm GK}(q). \tag{12}$$

The friction provides the dissipation of collective motion energy into internal energy. The fluctuations in the system are described by the random force $g_{\mu\nu}\xi_\nu$. Here ξ_ν is a random number with the following properties:

$$\langle \xi_\nu \rangle = 0,$$
$$\langle \xi_\mu(t_1)\xi_\nu(t_2)\rangle = 2\delta_{\mu\nu}\delta(t_1 - t_2). \tag{13}$$

The magnitude of the random force $g_{\mu\nu}$ is expressed in terms of diffusion tensor $D_{\mu\nu}$, $D_{\mu\nu} = g_{\mu\eta}g_{\eta\nu}$, which is related to the friction tensor $\gamma_{\mu\nu}$ via the modified Einstein relation $D_{\mu\nu} = T^*\gamma_{\mu\nu}$, where T^* is the effective temperature [16],

$$T^* = \frac{\hbar\varpi}{2}\coth\frac{\hbar\varpi}{2T}. \tag{14}$$

The parameter ϖ is the local frequency of collective motion [16]. The minimum of T^* is given by $\hbar\varpi/2$.

The total energy of the system is fixed at the initial stage,

$$E_{\rm tot} = E^{(t)}_{\rm g.s.} + E^{(p)}_{\rm g.s.} + E_{\rm c.m.}. \tag{15}$$

Here $E^{(t)}_{\rm g.s.}$, $E^{(p)}_{\rm g.s.}$ are the ground-state energies of the target and projectile, $E_{\rm c.m.} = E_{\rm lab}A_{\rm p}/(A_{\rm p} + A_{\rm t})$ is the energy of relative motion of target and projectile, calculated in the center-of-mass system, and $A_{\rm p}$ and $A_{\rm t}$ are, correspondingly, the mass numbers of the target and projectile. By introducing the Q value of the reaction,

$$Q \equiv E^{(t)}_{\rm g.s.} + E^{(p)}_{\rm g.s.} - E^{(t+p)}_{\rm g.s.}, \tag{16}$$

the total energy can be written as

$$E_{\rm tot} = E^{(t+p)}_{\rm g.s.} + E_x \quad \text{with} \quad E_x = E_{\rm c.m.} + Q. \tag{17}$$

E_x is the excitation energy of the system above the ground state of the compound nucleus formed after fusion of target and projectile. E_x is fixed by the initial conditions and does not depend on time. The calculations in the present work were carried out for the few values of E_x mentioned below.

Some terms of Eqs. (1) should be determined twice, ones for the first, and ones for the second stage of calculations. Such terms we denote by the upper indexes (I) and (II), respectively.

A. The entrance channel

In the entrance channel, we describe the process of collision of an initially spherical projectile nucleus and a deformed target nucleus. During the approaching process the projectile also gets deformed (spheroidal).

To fix the shape of such a system (Fig. 2), it is necessary to use at least four parameters (four collective coordinates), $\mathbf{q} \equiv (r, \alpha_t, \alpha_p, \theta_t)$.

The potential energy of the system in the entrance channel includes the energy of the Coulomb [17] and nuclear interactions [18], adopted for the collision of the deformed nuclei [5,19], its rotational energy [20], as well as the deformation energy of each nuclei,

$$V^I_{\rm pot} = V_{\rm Coul} + V_{\rm GK} + E^I_{\rm rot} + E^{(t)}_{\rm def} + E^{(p)}_{\rm def}. \tag{18}$$

The method for the calculation of the Coulomb interaction energy, developed in Ref. [17], takes into account both the deformation and the orientations of the ions. The calculation of the nuclear interactions $V_{\rm GK}$ is explained in Ref. [21]. The angular moment L in the rotational energy is considered as a fixed parameter.

The dependence of the potential energy of the system on the parameter r is shown in Fig. 3. The dotted horizontal lines in this figure are the reaction energies $E_x = 57.7, 47.3,$

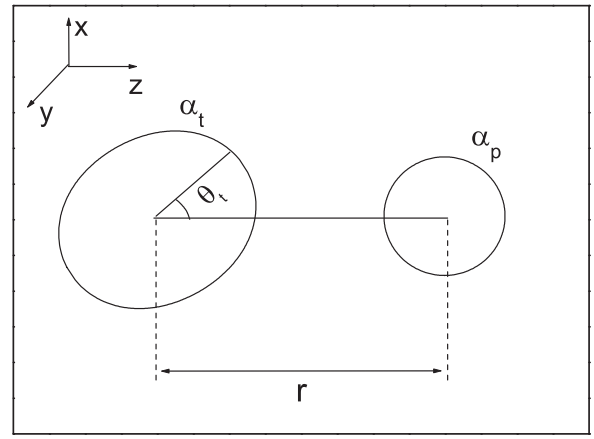

FIG. 2. Collective coordinates of the system, which consist of two separated nuclei. The shape of the system is determined by four parameters, namely, by the distance r between the centers of mass of the colliding nuclei, by the deformation parameters of the target (α_t) and projectile (α_p) nuclei, and by the orientational parameter θ_t, which is an angle between the symmetrical axis of the deformed in the ground-state target nucleus and the line connecting centers of mass of the colliding nuclei.

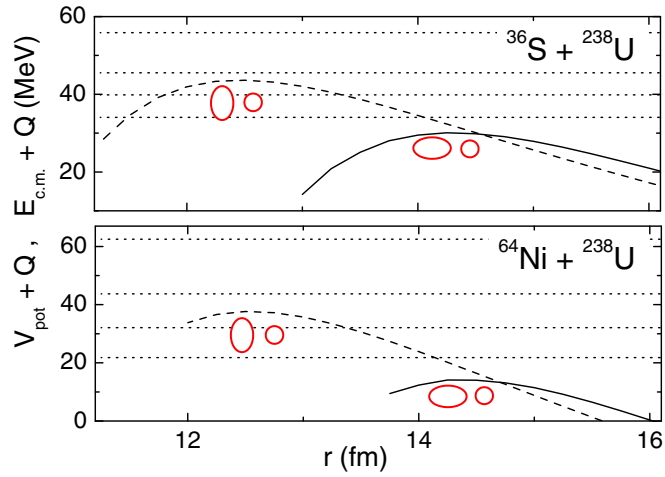

FIG. 3. The potential energy $V^I_{\rm pot}$ (18) of colliding ions ^{36}S + ^{238}U and ^{64}Ni + ^{238}U in the fusion channel for $L = 0$, $\theta_t = 0$ (solid) and $\theta_t = 90^{\rm o}$ (dashed). Dotted horizontal lines are the reaction energy $E_x = E_{\rm cm} + Q$.

41.6, 35.8 MeV for the $^{36}S + ^{238}U$ reaction, and $E_x = 64.1$, 45.1, 33.5, 23.2 MeV for the $^{64}Ni + ^{238}U$ reaction, at which the fission and quasifission of the composite systems with $Z = 108, 120$ were investigated in Ref. [22]. From this figure, it is clear that the height of the Coulomb barrier depends very much on the orientation of the target nucleus.

The initial value of r is chosen by the requirement that the nuclear interaction can be neglected and the Coulomb interaction between ions does not depend on their deformations and mutual orientation. The value $r = 50$ fm used in this paper satisfies these criteria well. The initial orientation of the target nucleus is distributed randomly, and the initial shape of the target nucleus corresponds to its ground state. At the initial moment of time, the movement in the system occurs only along the radial coordinate.

Starting with the initial value of collective variables and solving the equations of motion (1), one can determine the shape parameters of the system and the corresponding momentum at the next moments of time.

The exchange of energy between the collective and the single-particle degrees of freedom in the system being considered is induced both by the relative motion of colliding nuclei and by their deformation. Quantitatively, the exchange of energy is characterized by the mass and friction tensors.

The deformation of target and projectile are determined by one parameter, α_t or α_p. Thus, all four collective parameters in the entrance channel are "orthogonal" to each other, i.e., the mass and inverse-mass tensors are diagonal with respect to all four parameters. The diagonal components of the mass tensor describe the inertia of the system with respect to the motion along the corresponding degrees of freedom; namely, inertia of the system with respect to the radial motion is described by its reduced mass M, the inertia of the system with respect to the deformation of each of the nucleus is described by mass $m^I_{\mu\nu}$ tensors of the isolated deformed nucleus [they were specified above in Eq. (5)], the inertia of the system with respect to the rotation of the deformed target nucleus is described by its rigid-body moment of inertia J_t arbitrarily oriented in space.

To determine components of the friction tensor we use the equation

$$\gamma_{\mu\nu} = \gamma^{\rm fus}_{\mu\nu} + \delta_{\mu\alpha_t}\delta_{\alpha_t\nu}\gamma^I_{\alpha_t\alpha_t} + \delta_{\mu\alpha_p}\delta_{\alpha_p\nu}\gamma^I_{\alpha_p\alpha_p}. \tag{19}$$

The first term $\gamma^{\rm fus}_{\mu\nu}$ in this equation is determined in accordance with the surface-friction model [19]. It depends on relative motion of the colliding nuclei. The second and third terms are components of the friction $\gamma^I_{\alpha\mu}$ tensor of isolated deformed target and projectile nuclei [specified above in Eqs. (4)]. So, in the same way as done in Ref. [23], diagonal components of the friction tensor responsible for energy dissipation during the deformation of each of the nuclei are summed with the corresponding components obtained in the linear-response theory.

Due to the presence in the Langevin equations of the random force term, starting the calculation from the same point in the space of deformation parameters, one can get an infinitely large number of possible variants of the evolution of the system (similar to the trajectories of a Brownian particle in the space of collective coordinates describing the state of the system).

For the fixed value of the angular momentum of the system, L, the heights of Coulomb barriers will be different for different trajectories. Part of the trajectories will be reflected by the Coulomb barrier. Part of the trajectories $N_{\rm bar}(L)$ will overcome the barrier. Knowing the initial number of trajectories $N(L)$ with angular momentum L, we can find the probability and cross sections [partial $\sigma_{\rm bar}(L)$ and full $\sigma_{\rm bar}$] of crossing the Coulomb barrier:

$$\begin{aligned} P_{\rm bar}(L) &= N_{\rm bar}(L)/N(L), \\ \sigma_{\rm bar}(L) &= (\pi/k^2)(2L+1)P_{\rm bar}(L), \\ \sigma_{\rm bar} &= \sum_L \sigma_{\rm bar}(L), \end{aligned} \tag{20}$$

where k^2 is given by $k^2 = 2ME_{\rm c.m.}/\hbar^2$ with M being the reduced mass in the entrance channel and $E_{\rm c.m.}$ being the incident energy in the center-of-mass frame. The first-stage calculations are stopped at the moment when the system passes through the Coulomb barrier or reaches the internal turning point for the subbarrier fusion. The values of the deformation parameters of the system, as well as the values of potential, kinetic, and internal energy, are recorded. So, the distance between the centers of mass of the colliding nuclei r depends on the point at which the system crossed the Coulomb barrier. With this information, we begin to describe the evolution of a highly deformed system formed after touching of the initial nuclei.

B. Transition procedure

The system formed after the touching of colliding nuclei is a highly deformed mass-asymmetric system with a well-pronounced neck. To describe the shape of such systems, one needs to introduce at least three parameters that are responsible for the thickness of the neck, the distribution of the mass relative to the neck, and the elongation of the entire system. In the shape parametrization used in the present work and based on Cassini ovaloids, we consider three deformation parameters α, α_1, α_4 that regulate the total elongation, the mass asymmetry, and the neck radius, respectively.

The two of these parameters (α, α_1) can be found from the requirement that elongation and the mass asymmetry of the compact system are the same as that of two ions at the touching point. Unfortunately, the neck parameter for the touching system is not defined. So, it was assumed in Ref. [24] that the compact system attains the shape that corresponds to the minimum of deformation energy with respect to α_4 (for given α and α_1). The demonstration of the definition of α_4 by such a procedure is presented in Fig. 4.

To set the initial values for the momenta we transform the kinetic energy in the r direction into the kinetic energy in α direction, $E^{(rr)}_{kin} = p^2_\alpha/2m_{\alpha\alpha}(\alpha, \alpha_1, \alpha_4)$. The rest of the initial kinetic energy is shared randomly between the α_1 and α_4 degrees of freedom.

C. The evolution of combined system

After the initial parameters of the mono-system are set, we start solving the Langevin equations (1). The potential energy

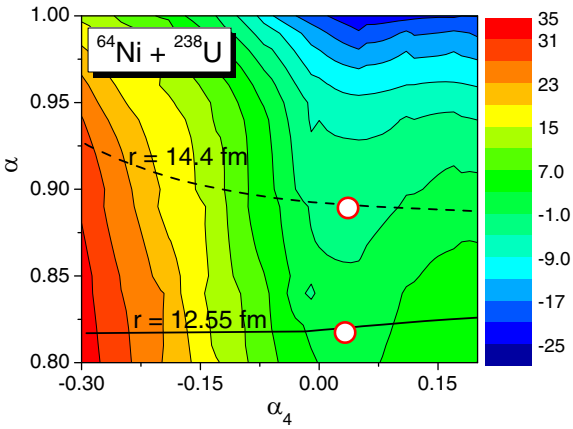

FIG. 4. The deformation energy $E_{\rm def}$ at $T = 0$ of the combined system formed in the reaction ^{64}Ni + ^{238}U as a function of the parameters α_4 and α (α_1 is fixed by the mass asymmetry of ^{64}Ni + ^{238}U) system. The dashed line corresponds to fixed distance $r = 14.4$ fm between the centers of mass of ions for the nose-to-nose touching configuration, and the solid line ($r = 12.55$) corresponds to side-to-side configuration (see Fig. 3). The circle marks the point where potential energy is minimal with respect to variations of α_4.

of the system included in these equations is the sum of the deformation and rotation energies,

$$V^{II}_{\rm pot} = E_{\rm def} + E^{II}_{\rm rot}. \tag{21}$$

Tensors $\gamma_{\mu\nu}$ and $m_{\mu\nu}$ [Eqs. (4) and (5)] characterize completely the inertia and friction properties of the combined system.

After the start of calculations, all collective parameters of the system can change, directing it either to the ground state or to the scission line. The main change, however, is along with the mass asymmetric coordinate α_1. The outcome of the Langevin equations depends very much on how much the mass asymmetric coordinate has changed before the fission.

If masses of separated parts of the system did not change much from the masses of colliding ions, then the deep-inelastic collisions occur. If the masses change much, then such events correspond to fission or quasifission events. The latter differ from each other in how close the system came to the ground state before the separation occurred.

In the Figs. 5 and 6 we show the dependence of deformation energy ($L = 0$) of synthesized nuclei ^{302}120 and ^{274}Hs on the parameters α è α_1 ($\alpha_4 = 0$). The initial deformation of the mono-system for ^{302}120 and ^{274}Hs is marked by circles. Possible directions of its evolution are shown by arrows. It is clearly seen that, in the case of ^{274}Hs, the system has more chances to come to the ground state compared with ^{302}120.

During the evolution of the combined system, the total energy $E_{\rm tot}$ is shared between the local potential, kinetic, and excitation energies:

$$E_{\rm tot} = V_{\rm pot}(q) + E_{\rm kin}(q) + E^*(q). \tag{22}$$

Taking into account Eq. (17) for $E_{\rm tot}$, the local excitation energy is brought to the form

$$E^*(q) = E_x - \left[V_{\rm pot}(q) - E^{(t+p)}_{\rm g.s.}\right] - E_{\rm kin}(q). \tag{23}$$

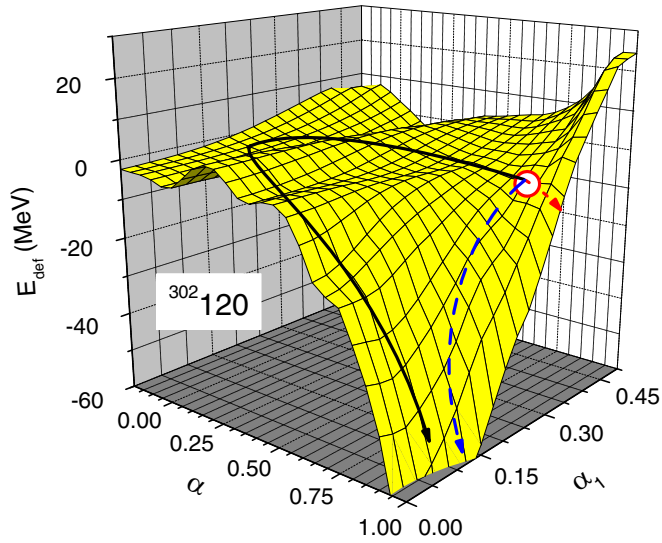

FIG. 5. The dependence of the potential energy of the system ^{302}120 on the parameters α and α_1 ($\alpha_4 = 0$). The circle shows the approximate position of the initial point of evolution of the mono-system formed in the reaction ^{64}Ni + ^{238}U. The arrows show the possible directions of evolution of the mono-system: dot: deep-inelastic collision, dashes: quasifission, solid: fission.

Note that the local excitation energy $E^*(q)$ does not coincide with E_x. The probability of particles or γ-quanta emission and the kinetic energies of emitted particles is defined mainly by the local excitation energy $E^*(q)$. With some probability, the system could also avoid fission and form the evaporation residue. This event is realized if the system being near the ground state will reduce its excitation energy by evaporating light particles (primarily neutrons) or emitting γ rays. The probability of these processes is estimated in the framework of the statistical model [15] at each step of the integration of Langevin equations (1).

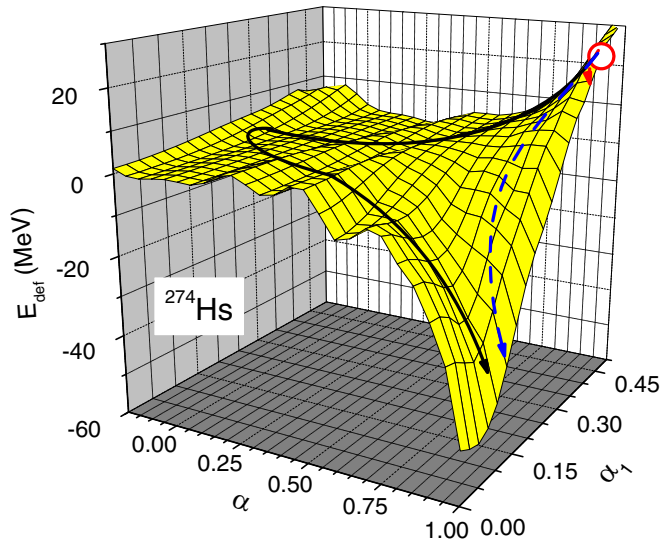

FIG. 6. The same as in Fig. 5, but for the ^{274}Hs nucleus, formed in the reaction ^{36}S + ^{238}U.

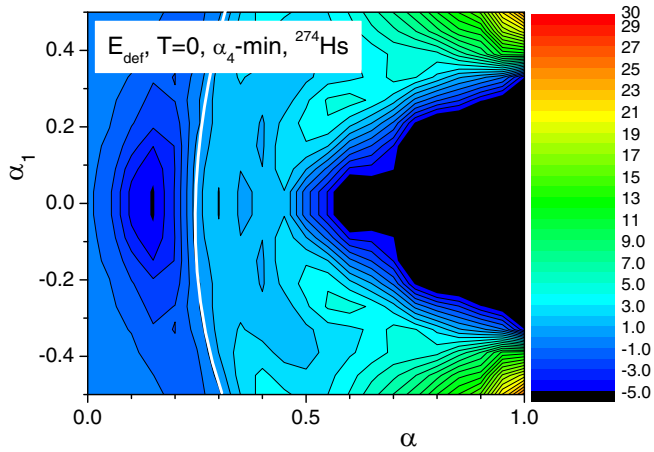

FIG. 7. The deformation energy of ^{274}Th at $T = 0$ minimized with respect to α_4. The white line marks the position of the fission barrier.

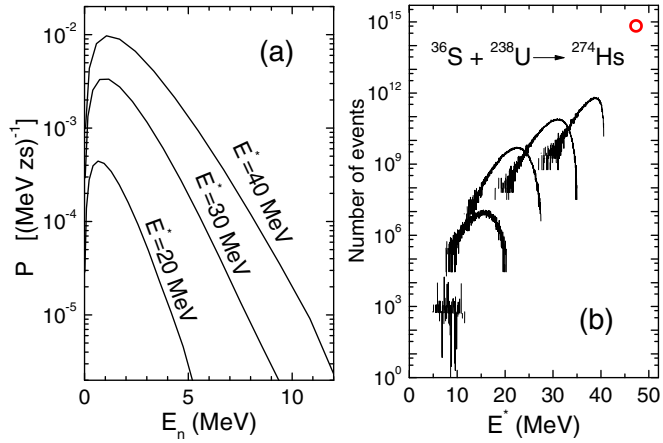

FIG. 8. (a) The probability $P(E_n)$ [Eq. (25)] of neutron emission per time unit as a function of neutron kinetic energy E_n for a few values of excitation energy E^* of compound nucleus ^{274}Hs. (b) The dependence of the number of trajectories that stay at the ground-state region ($\alpha \leqslant 0.1$) after emission of 1, 2, 3, 4, and 5 neutrons on the excitation energy E^* of the compound nucleus. The initial excitation energy $E^* = 47.3$ MeV is marked by the circle.

We calculate the evolution of the compact system either until it crosses the fission barrier (white line in Fig. 7) back and splits into two fragments or until it gets deexcited by the emission of light particles and γ rays and forms the evaporation residue.

To form the evaporation residue, the system should release the excitation energy by the evaporation of light particles and γ quanta. We describe the particle evaporation from an excited nucleus by the statistical method proposed in Ref. [15], see also Ref. [20]. On each step of the integration of Langevin equations by the hit-and-miss method, we check if the particle was emitted and what kind of partible was emitted. The expressions for the evaporation widths Γ_j ($j \equiv n$, p, d, t, ^{3}He, α) and Γ_γ are given in Ref. [15]. In particular, for the probability P_n of emitting neutron within the time step Δt of integration of Langevin equations one can find

$$P_n = \Delta t \int_0^{E_n^* - B_n} P(E_n) dE_n, \tag{24}$$

where $P(E_n)$ is the probability of emitting a neutron with a certain energy E_n per time and energy units,

$$P(E_n) = \frac{(2s_n + 1)m_n}{\pi^2 \hbar^3 \rho_0(E_0^*)} \sigma_{inv}(E_n) E_n \rho_n(E_n^* - B_n - E_n). \tag{25}$$

Here, ρ_0 and ρ_n are the level densities in the primary nucleus and the nucleus formed after neutron emission; s_n, m_n, B_n are the spin of the emitted neutron, its mass, and its binding energy, respectively; $\sigma_{inv}(E_n)$ is the cross section for the absorption of a neutron with kinetic energy E_n by the considered nucleus; $E_n^* = E^* - \Delta_n$; $E_0^* = E^* - \Delta_0$; E^* is the compound-nucleus excitation energy; and Δ_n and Δ_0 are the pairing gaps for the residual and the primary nucleus, respectively. The probability P_n for the ^{274}Hs nucleus is shown in Fig. 8(a). After finding the sum of probabilities to evaporate any particle (total probability), which is calculated in the same way as demonstrated here for neutrons (24), by the hit-and-miss method we determine which particle, if any, was evaporated. For this, we generate a random number ξ between zero and unity and compare it with the total probability. If this random number is smaller than the total probability, it is assumed that a particle is emitted at the current step of solving Langevin equations. The kind of a particle is determined again at random proportionally to the known probability of evaporation of any particle. Then, knowing the dependence of the particle evaporation probability on its kinetic energy, we again randomly choose its kinetic energy. As one can see from Fig. 8(a), the most probable kinetic energy of the evaporated neutrons is close to 1–2 MeV.

If some particle is emitted, the binding energy of this particle is subtracted from the excitation energy of the system, the deformation energy, and the transport coefficient are replaced by these for smaller particle number. The calculations show that, at high value of E_x, $E_x \approx 50$ MeV up to 4 to 5 neutrons can be emitted.

During the evolution of the system from the touching configuration, it has a very high probability to split into two pieces and form the product of quasifission. A very few trajectories would reach the ground-state deformation. Some of them could decrease their excitation energy by light particles or gamma emissions. The dependence of the probability to come to the ground state on the number of evaporated neutrons will be discussed in the next section. Here we illustrate the deexcitation process and evaporation residue formation in the reaction $^{36}\mathrm{S} + ^{238}\mathrm{U} \rightarrow ^{274}\mathrm{Hs}$ for the case when trajectories come to the ground state without evaporation of any particles with their initial energy $E_x = 47.3$ MeV. Figure 8(b) demonstrates the deexcitation process. The "survived" nuclei could reduce the excitation energy by the first evaporation of neutron. Since the kinetic energy of first emitted neutron is not fixed but distributed around some most probable value, see Fig. 8(a), after neutron emission, one gets the distribution of events around the most probable excitation energy $E^* = 38.7$ MeV [first peak on the right in Fig. 8(b)]. The

excitation energy after evaporation of the first neutron is still high, the main fraction of nuclei would fission, the rest would emit the second neutron and form the second peak on the right in Fig. 8(b) with the most probable excitation energy $E^* = 31.0$ MeV. The process of fission and neutron emission would continue until the excitation energy becomes smaller than the fission barrier. In this case, one can say that the evaporation residue was formed. The number of trajectories that formed the evaporation residue in the case of ^{274}Hs is by 13–15 orders of magnitude smaller than the initial number of trajectories that reached the ground state.

Knowing probability of the system formed after collision of the initial nuclei to form the compound nucleus (fusion process), $P_{\rm CN}(L)$, and the probability for the compound nucleus to survive against fission, $W_{\rm sur}(L)$, one can calculate fusion $\sigma_{\rm fus}$ and evaporation residue formation $\sigma_{\rm er}$ cross sections:

$$\sigma_{\rm fus} = \sum_L \sigma_{\rm fus}(L) = \sum_L \sigma_{\rm bar}(L) P_{\rm CN}(L) \tag{26}$$

and

$$\sigma_{\rm er} = \sum_L \sigma_{\rm er}(L) = \sum_L \sigma_{\rm bar}(L) P_{\rm CN}(L) W_{\rm sur}(L), \tag{27}$$

where $\sigma_{\rm fus}(L)$ and $\sigma_{\rm er}(L)$ are fusion and evaporation residue formation partial cross sections, respectively.

To have reliable results (at least 10^5 events of evaporation residue formation) we should calculate about 10^{18}–10^{24} trajectories (the number of trajectories depends on the reaction and its energy). Of course, it is impossible to run such a number of trajectories. So, we use some simplified procedure. In the entrance channel, we consider 10^6 trajectories. Approximately 10% of these would reach the touching point. In other words, at the beginning of the second stage of calculations we have 10^5 trajectories. We run each trajectory ten times. So, initially, at the beginning of the second stage of calculation, we have again 10^6 trajectories. The majority of these trajectories would undergo fission (cross the line $\alpha = 1.0$). We continue the calculations until only 10% would remain at the compact shape. Then, from the endpoint of each of the survived 10^5 trajectories, using data of its coordinates and momenta, we start the calculations ten times. So, we again have 10^6 trajectories. Repeating this procedure, again and again, we finally obtain 10^5 events of evaporation residue formation.

III. RESULTS AND DISCUSSIONS

In the present work we consider the fusion-fission process in reactions $^{36}\mathrm{S} + ^{238}\mathrm{U} \to ^{274}\mathrm{Hs}$ and $^{64}\mathrm{Ni} + ^{238}\mathrm{U} \to ^{302}120$. The calculations of the entrance channel provide for these reactions the Coulomb barrier penetration cross sections. Their values should be close to the values of the capture cross sections obtained in experiments. It should be noted that the probability of capture is determined by the probability that fission or quasifission events occur during the reaction. And it does not include the probability of a deep-inelastic scattering process, which, in principle, can occur at the second stage of the reaction. Therefore, the cross sections of the system crossing the Coulomb barrier obtained at the end of the first stage of calculation may be slightly larger than the capture cross sections.

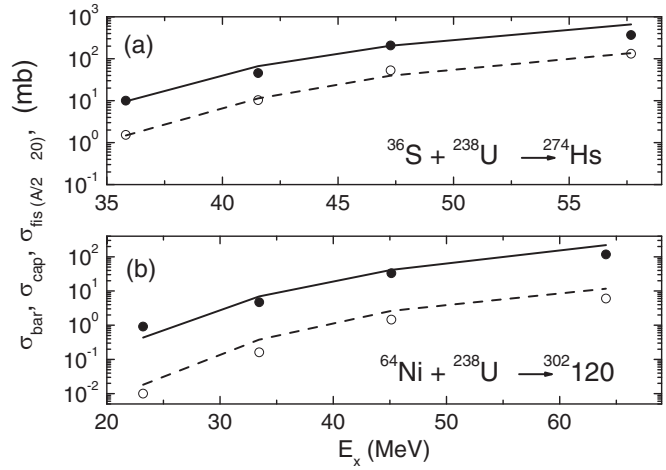

FIG. 9. The Coulomb barrier penetration cross sections (solid line) for the reaction (a) $^{36}\mathrm{S} + ^{238}\mathrm{U}$ and (b) $^{64}\mathrm{Ni} + ^{238}\mathrm{U}$ as function of the reaction energy $E_x = E_{\rm c.m.} + Q$. Closed circles are the experimental data on capture cross sections [22]. The cross sections of the fission of the compact system, corresponding to the fragment mass asymmetry $A/2 \pm 20$ are shown by the dashed line (calculations) and open circles (experimental data [22]).

Figure 9 gives the cross sections of the Coulomb barrier penetration, and the cross sections of the almost-symmetric (with the ratio of the masses of fragments $A/2 \pm 20$) fission and quasifission of the system, formed after touching of the initial nuclei. For comparison, the corresponding experimental data [22] are also presented. It can be seen that the theoretical calculations agree rather well with the experimental data.

It would be interesting to know which contribution to fission events comes from true fission and which contribution comes from quasifission. For this we calculated the number of trajectories that cross the barrier (for ^{274}Hs see white line in Fig. 7) from outside. As one could expect, this number is very small, only 10^{-4} for ^{274}Hs and from 10^{-6} to 10^{-5} for $^{302}120$ depending on the excitation energy E_x. Thus, almost all contributions to the mass distributions of fission fragments in fusion-fission reactions with SHEs comes from the quasifission process.

The fraction of trajectories that do not undergo quasifission immediately and can reach the region of the ground-state deformation is very small. Such trajectories can be considered as leading to the fusion of the colliding ions. During further evolution, the mono-system can evaporate few neutrons or γ rays. So, the compound nucleus will be a set of different isotopes with different excitation energies.

The values of fusion cross sections (events reaching the ground state), for all considered energies of reaction $^{36}\mathrm{S} + ^{238}\mathrm{U} \to ^{274-x}\mathrm{Hs} + xn$ and $^{64}\mathrm{Ni} + ^{238}\mathrm{U} \to ^{302-x}120 + xn$, are given in Fig. 10.

The obtained results for the fusion cross sections and the excitation energies of the corresponding isotopes can be used for calculation of the evaporation residues formation cross

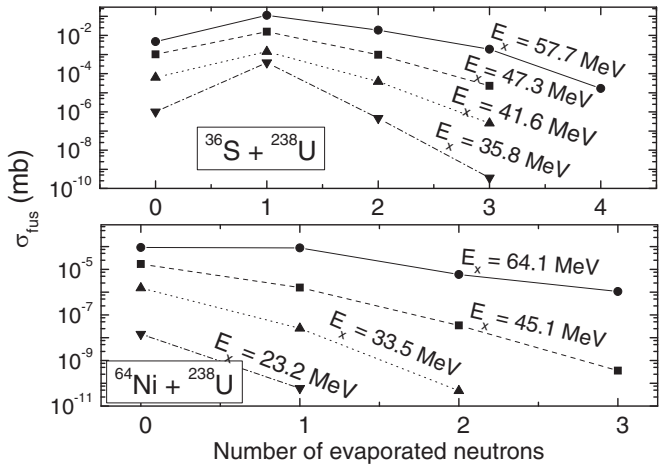

FIG. 10. The dependence of fusion cross section, obtained for the reaction $^{36}\mathrm{S}+^{238}\mathrm{U}\rightarrow{}^{274-x}\mathrm{Hs}+xn$ and $^{64}\mathrm{Ni}+^{238}\mathrm{U}\rightarrow{}^{302-x}120+xn$, on the number of emitted neutrons.

sections. The summed over all isotopes values of the fusion cross sections and the evaporation residue formation cross sections are given in Fig. 11.

The first superheavy element with $Z=108$, ^{266}Hs, was synthesized at GSI, Darmstadt [25] in the so-called cold fusion reaction $^{58}\mathrm{Fe}+{}^{208}\mathrm{Pb}\rightarrow{}^{266}\mathrm{Hs}$ with the doubly magic ^{208}Pb as a target. The excitation energy of the compound system in this reaction was rather low 18 ± 2 MeV and only one neutron was emitted during the deexcitation process. For the three observed events, the production cross section $\sigma_{\mathrm{er}}=19^{+18}_{-11}$ pb was deduced.

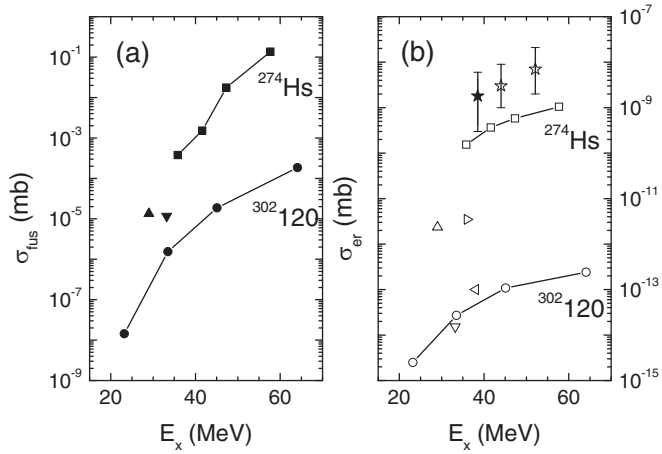

FIG. 11. (a) The dependence of the total fusion cross sections of the isotopes obtained in the reactions $^{36}\mathrm{S}+^{238}\mathrm{U}\rightarrow{}^{274}\mathrm{Hs}$ and $^{64}\mathrm{Ni}+^{238}\mathrm{U}\rightarrow{}^{302}120$ on the initial excitation energy E_x. The triangles are the results from Ref. [28] at $E_x=29.0$ MeV (▲) and $E_x=33.2$ MeV (▼). (b) The evaporation residues formation cross sections for the same reactions. The up (△) and down (▽) triangles mark the data obtained in Ref. [28]. The right triangle, the stars, and the left triangle are the results from Refs. [29] (▷), [26] (⋆), and [27,30] (◁).

The heavier superheavies $Z=114-118$ were produced at the Joint Institute for Nuclear Research in Dubna in the so-called warm fusion reactions. In these reactions, the initial excitation of the compound nucleus was of the order of 30–40 MeV, consequently, up to 4 to 5 neutrons were emitted and the residue formation cross section was much lower as compared with the cold fusion reactions. For the comparison of our calculated results for ^{274}Hs, we choose the available experimental results from similar reactions $^{34}\mathrm{S}+{}^{238}\mathrm{U}\rightarrow{}^{272}\mathrm{Hs}$ at $E_x=38.5$ MeV [26] and $^{26}\mathrm{Mg}+{}^{248}\mathrm{Cm}\rightarrow{}^{270}\mathrm{Hs}$, at $E_x=44$ MeV and $E_x=52.1$ MeV [27]. The last reaction is more mass-asymmetric than calculated here, so the higher values of σ_{er} than ours should be expected.

As one can see from the top part of Fig. 11(b) both experimental and calculated results grow with the increasing excitation energy E_x. The calculated results for $^{36}\mathrm{S}+{}^{238}\mathrm{U}\rightarrow{}^{274}\mathrm{Hs}$ reaction are on average by one order of magnitude smaller than the experimental cross sections from the reactions mentioned above.

The calculated data for the $^{64}\mathrm{Ni}+{}^{238}\mathrm{U}\rightarrow{}^{302}120$ reaction are shown in the bottom part of Fig. 11. As one could expect, the fusion cross section for $^{302}120$ is a few orders of magnitude smaller than that of ^{274}Hs. Consequently, the evaporation residue formation cross section σ_{er} for $^{302}120$ is also much smaller than that of ^{274}Hs.

For the comparison we show the results of time-dependent Hartree-Fock plus Langevin approach for hot fusion reactions [28] for more mass-asymmetric combinations of the target and projectile, $^{254}\mathrm{Fm}+{}^{48}\mathrm{Ca}$, $P_{\mathrm{CN}}W_{\mathrm{sur}}=302\times10^{-13}$ at $E_x=29.0$ MeV [up-triangle in Fig. 11(b)] and $^{248}\mathrm{Cm}+{}^{54}\mathrm{Cr}$, $P_{\mathrm{CN}}W_{\mathrm{sur}}=2.47\times10^{-13}$ at $E_x=33.2$ MeV (down-triangle). To bring the probabilities shown in Table 1 of Ref. [28] to the same dimension as our calculated cross sections we have multiplied the probabilities of Ref. [28] by the factor π/k^2, see Eq. (20). Unfortunately, in Ref. [28] the results of calculations are presented only for the case $L=0$, one term in the sum [see Eq. (27)]. The account of higher orbital momenta should increase the value of this sum. Thus, the calculations within the model of Ref. [28] for higher orbital momenta are very much desirable.

The right triangle ▷ shows the evaporation residue cross section calculated for the reaction $^{64}\mathrm{Ni}+{}^{238}\mathrm{U}\rightarrow{}^{302}120$ at $E_x=36$ MeV in dynamical (up to compound nucleus formation) statistical (survival probability calculations) model [29]. The left triangle ◁ is the evaporation residue cross section calculated in the recent work [30] for the same reaction at $E_x=38$ MeV within the microscopic-macroscopic approach [31] with the effective single-particle potentials obtained for the SHE from the self-consistent HFB calculations. Our calculated results [open circles in Fig. 11(b)] are in the middle between the calculations of Ref. [28–30], which is quite reasonable.

IV. CONCLUSIONS

In the present work, reactions that differ from each other by the ratio of the masses of colliding nuclei almost twice were studied. We have applied a dynamical approach to calculate the evolution of the system starting from the approaching of

the colliding ions to each other and up to fission (quasifission) of the system, formed after touching of the initial nuclei or up to the evaporation residue formation. The calculated evaporation residue formation cross sections for Hassium isotopes are by one order of magnitude smaller as compared with the existing experimental data. Thus, the values of the fusion cross sections and the evaporation residues formation cross section obtained for the reaction $^{64}\mathrm{Ni} + {}^{238}\mathrm{U} \rightarrow {}^{302-x}120 + xn$ should be considered with the same accuracy. Our results are in between the calculated results by Sekizawa (2019), Zagrebaev (2008), and Adamian (2020). According to our results, the most favorable energy of ^{64}Ni ions should be close to $E_{\mathrm{c.m.}} = 300$ MeV.

ACKNOWLEDGMENTS

One of us (V.L.) would like to express his gratitude to the Research Laboratory for Nuclear Reactors, Tokyo Institute of Technology, for the hospitality during his stay in Japan.

[1] V. L. Litnevsky, G. I. Kosenko, and F. A. Ivanyuk, Phys. Rev. C **93**, 064606 (2016).
[2] C. Shen, G. Kosenko, and Y. Abe, Phys. Rev. C **66**, 061602(R) (2002).
[3] G. I. Kosenko, F. A. Ivanyuk, and V. V. Pashkevich, J. Nucl. Radiochem. Sci. **3**, 71 (2002).
[4] Y. Abe, S. Ayik, P.-G. Reinhard, and E. Suraud, Phys. Rep. **275**, 49 (1996).
[5] J. Marten and P. Fröbrich, Nucl. Phys. A **545**, 854 (1992).
[6] V. V. Pashkevich, Nucl. Phys. A **169**, 275 (1971).
[7] W. D. Myers and W. J. Swiatecki, Nucl. Phys. **81**, 1 (1966).
[8] V. M. Strutinsky, Nucl. Phys. A **95**, 420 (1967).
[9] M. Brack, J. Damgaard, A. S. Jensen, H. C. Pauli, V. M. Strutinsky, and C. Y. Wong, Rev. Mod. Phys. **44**, 320 (1972).
[10] H. Hofmann, Phys. Rep. **284**, 137 (1997).
[11] H. Hofmann, *The Physics of Warm Nuclei With Analogies to Mesoscopic Systems* (Oxford University Press Inc., New York, 2008).
[12] F. A. Ivanyuk and H. Hofmann, Nucl. Phys. A **657**, 19 (1999).
[13] F. A. Ivanyuk, in *Proceedings of International Conference on Nuclear Physics "Nuclear Shells-50," Dubna, Russia, 21–24 April, 1999* (World Scientific, Singapore, 2000), p. 456.
[14] A. V. Ignatyuk, G. N. Smirenkin, and A. S. Tishin, Sov. J. Nucl. Phys. **21**, 255 (1975).
[15] A. S. Iljinov, M. V. Mebel, N. Bianchi, E. De Sanctis, C. Guaraldo, V. Lucherini, V. Muccifora, E. Polli, A. R. Reolon, and P. Rossi, Nucl. Phys. A **543**, 517 (1992).
[16] H. Hofmann and D. Kiderlen, Int. J. Mod. Phys. E **7**, 243 (1998).
[17] R. S. Kurmanov and G. I. Kosenko, Phys. At. Nucl. **77**, 1442 (2014).
[18] D. H. E. Gross and H. Kalinowski, Phys. Rep. **45**, 175 (1978).
[19] P. Fröbrich, Phys. Rep. **116**, 337 (1984).
[20] G. I. Kosenko, F. A. Ivanyuk, V. V. Pashkevich, and D. V. Dinner, Phys. At. Nucl. **71**, 2052 (2008).
[21] V. L. Litnevsky, G. I. Kosenko, and F. A. Ivanyuk, Phys. At. Nucl. **79**, 342 (2016).
[22] E. M. Kozulin, G. N. Knyazheva, K. V. Novikov, I. M. Itkis, M. G. Itkis, S. N. Dmitriev, Yu. Ts. Oganessian, A. A. Bogachev, N. I. Kozulina, I. Harca, W. H. Trzaska, and T. K. Ghosh, Phys. Rev. C **94**, 054613 (2016).
[23] V. L. Litnevsky, G. I. Kosenko, F. A. Ivanyuk, and V. V. Pashkevich, Phys. At. Nucl. **75**, 1500 (2012).
[24] V. L. Litnevsky, F. A. Ivanyuk, G. I. Kosenko, and S. Chiba, Phys. Rev. C **99**, 054624 (2019).
[25] G. Münzenberg, P. Armbruster, H. Folger, F. P. Heßberger, S. Hofmann, J. Keller, K. Poppensieker, W. Reisdorf, K.-H. Schmidt, H.-J. Schött, M. E. Leino, and R. Hingmann, Z. Phys. A: At. Nucl. (1975) **317**, 235 (1984).
[26] K. Nishio, S. Hofmann, F. P. Hessberger, D. Ackermann, S. Antalic, Y. Aritomo, V. F. Comas, C. E. Dullmann, A. Gorshkov, R. Graeger, K. Hagino, S. Heinz, J. A. Heredia, K. Hirose, H. Ikezoe, J. Khuyagbaatar, B. Kindler, I. Kojouharov, B. Lommel, R. Mann *et al.*, Phys. Rev. C **82**, 024611 (2010).
[27] J. Dvorak, W. Brüchle, M. Chelnokov, R. Dressler, C. E. Dullmann, K. Eberhardt, V. Gorshkov, E. Jager, R. Krcken, A. Kuznetsov, Y. Nagame, F. Nebel, Z. Novackova, Z. Qin, M. Schädel, B. Schausten, E. Schimpf, A. Semchenkov, P. Thörle, A. Türler *et al.*, Phys. Rev. Lett. **97**, 242501 (2006).
[28] K. Sekizawa and K. Hagino, Phys. Rev. C **99**, 051602(R) (2019).
[29] V. Zagrebaev and W. Greiner, Phys. Rev. C **78**, 034610 (2008).
[30] G. G. Adamian, N. V. Antonenko, H. Lenske, and L. A. Malov, Phys. Rev. C **101**, 034301 (2020).
[31] G. G. Adamian, L. A. Malov, N. V. Antonenko, and R. V. Jolos, Phys. Rev. C **97**, 034308 (2018).